Theoretical Study of 5-phenyltropolone in the S_0 and S_1 States

Yukio Nishimura,* Takeshi Tsuji, and Hiroshi Sekiya†

Research Institute of Advanced Material Study, Kyushu University, Kasuga 816-8580, Japan

Received: February 17, 2001; In Final Form: May 21, 2001

The optimized geometry of 5-phenyltropolone (5PTRN) has been calculated by using the B3LYP/6-311+G(2d,p) method in the S_0 state. The seven-membered ring of the tropolone moiety deviates slightly from planarity. The equilibrium torsional dihedral angle in the S_0 state is determined to be ca. 44°, which is close to the experimental value for the isotopomer of 5PTRN, 5PTRN(−OD). There are two barriers for phenyl rotation at the torsional angles of 0° and 90°, in which the former barrier at 0° is higher than the latter one at 90°. The CIS calculation suggests that in the S_1 state, the deviation from planarity in the seven-membered ring of the tropolone moiety increases, and the barrier for phenyl rotation at the torsional angle of 0° is lower than that at 90°. Assignment of low-frequency bands is discussed based on the calculated vibrational fundamentals for the S_0 state.

1. Introduction

Hydrogen bonds play important roles in many chemical and biological phenomena. Tropolone (TRN) is a typical intramolecularly hydrogen-bonded molecule that undergoes proton tunneling. Such tunneling cannot be described by a one-dimensional model along the O···H···O coordinates. Much attention has been focused on the multidimensional features of tunneling. Substituents in the TRN ring exert great influence on proton tunneling. Substitution of a halogen atom at the 5-position of TRN (symmetrical substitution) has been reported to increase the tunneling splitting relative to that of TRN.[1] On the other hand, unsymmetrically substituted tropolones, such as 3-Cl-tropolone and 3-Br-tropolone, quenched proton tunneling and did not show any tunneling splitting under the jet-cooled conditions.[2,3]

It is interesting to know the effects of internal motion of substituents on the proton tunneling of TRN. Many studies have been performed to examine the torsional mode coupling effects of substituents in the proton tunneling of TRN.[4−11] In the ground state of 5-aminotropolone, intramolecular proton tunneling between equivalent minima has been reported to be accompanied by an internal rotation of the amino group.[4] Introduction of asymmetry by substituting one D atom into the NH_2 group quenched proton tunneling in the ground state.[4] These experimental findings have been supported by a combined ab initio + nuclear dynamic study.[9] In 5-hydroxytropolone, the two in-plane orientations of the 5-OH substituent produced two isomers, syn and anti, relative to the 2-OH.[5,6] It has been postulated that there are two reaction coordinates for the syn-anti photoisomerization; these coordinates involve 2-OH tunneling and 5-OH torsion.[6−8] Nishi et al. have clarified the coupling as regards the internal rotation of the methyl group and the intramolecular proton transfer.[10,11] They showed a drastic decrease in the tunneling splitting of the zero-vibrational level, compared to that of TRN.

5-Phenyltropolone (5PTRN) can assume different conformations depending on the internal rotation of the phenyl group, which would be coupled with proton tunneling. We have observed the electronic spectra of jet-cooled 5PTRN by exciting the S_0-S_1 transition.[12,13] Low-frequency bands due to phenyl torsion were observed in both the fluorescence excitation spectrum and the single vibronic level fluorescence spectrum. Proton tunneling was shown to be suppressed by phenyl torsion. One-dimensional torsional potential function analysis of low-frequency bands has been carried out in the S_0 state. That analysis suggested that there were two potential barriers for phenyl rotation at the torsional angles of 0° and 90°. Additional information about the structure of 5PTRN would be helpful for further discussion of proton tunneling. The present paper describes ab initio calculations of 5PTRN in the ground state (S_0) and in the first excited state (S_1). The calculations encompass determinations of the energies and fully optimized geometries in the S_0 and S_1 states; vibrational frequencies were determined for the S_0 state.

2. Calculation

All calculations were carried out with the GAUSSIAN 94 package[14] on a DEC/Alpha work station. For the study of the ground electronic state (S_0), the geometry optimization was performed using the B3LYP method[15a,b] at the 6-311+G(2d,p)[16] level. Energies of conformers formed by phenyl rotation were also computed in order to know the rotational barrier for the phenyl group. Vibrational frequencies for the S_0 state were calculated at the 6-31G** level, which includes a set of d-polarization orbitals for heavy atoms and a p set for hydrogens.[16] For the excited S_1 state, a configuration interaction of all single excitation method (CIS)[17] implemented in the GAUSSIAN 94 package was used for the geometry optimization and the energy determination. The geometry of the transiton state for proton transfer was optimized by the QST2 method for both the S_0 and the S_1 states.

3. Results and Discussion

3.1. Calculation of the S_0 State. *3.1.1 Optimized Geometry of TRN.* Since the structure of 5PTRN in the S_0 state has not

* To whom correspondence should be addressed. Present address: 7-18-35 Tounoharu, Higashiku, Fukuoka 813-0001, Japan.

† Department of Molecular Chemistry, Graduate School of Science, Kyushu University.

10.1021/jp010638c CCC: $20.00
Published on Web 07/04/2001

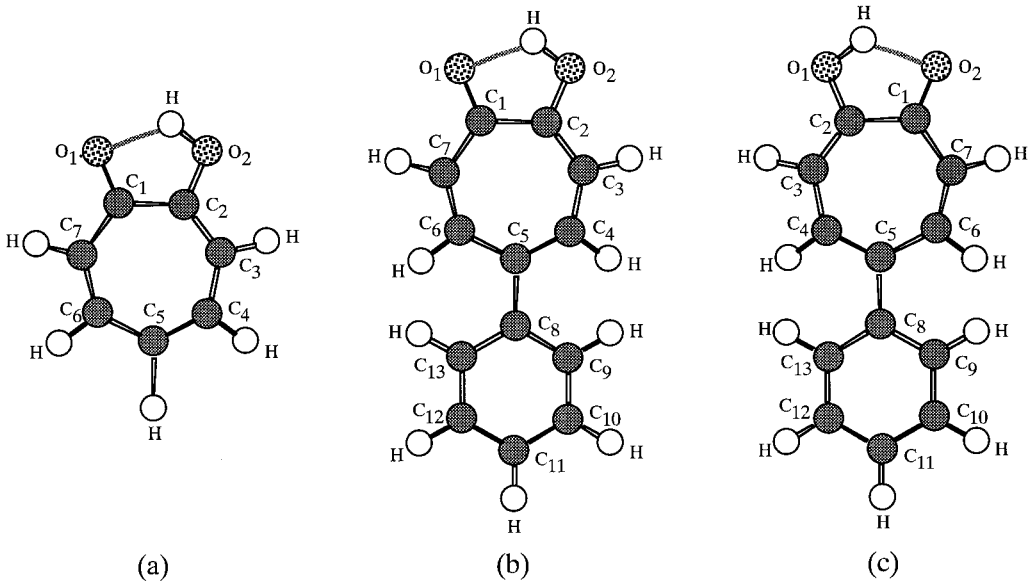

Figure 1. Numbering of carbon and oxygen atoms: (a) TRN, (b) the normal form of 5PTRN, (c) the tautomer of 5PTRN.

TABLE 1: Comparison of Bond Lengths and Angles of TRN between the Geometry Optimized by the B3LYP/6-311+G(2d,p) Method and Observed Geometry in the S_0 State

	bond length (Å)			bond angle (degree)	
	calcd	crystal[a]		calcd	crystal[a]
$C_1{=}O_1$	1.246	1.261	$C_2C_1{=}O_1$	114.7	115.4
$C_2{-}O_2$	1.331	1.333	$C_1C_2{-}O_2$	111.3	114.7
O_2H	0.992	0.94	$C_7C_1O_1$	121.9	120.4
C_1C_2	1.487	1.454	C_2O_2H	103.2	107
C_2C_3	1.372	1.379	$C_1C_2C_3$	130.0	128.8
C_3C_4	1.407	1.393	$C_2C_3C_4$	129.0	129.4
C_4C_5	1.373	1.341	$C_3C_4C_5$	129.4	129.9
C_5C_6	1.411	1.410	$C_4C_5C_6$	127.6	127.5
C_6C_7	1.370	1.373	$C_5C_6C_7$	130.4	129.4
C_7C_1	1.433	1.410	$C_6C_7C_1$	130.3	130.6
C_3H	1.085	1.09	$C_7C_1C_2$	123.3	124.2
C_4H	1.085	1.04	C_4C_3H	116.5	115
C_5H	1.084	1.07	C_5C_4H	116.0	116
C_6H	1.086	1.08	C_6C_5H	115.9	114
C_7H	1.085	1.09	C_7C_6H	114.9	115
$O_1{\cdots}O_2$	2.476	2.553	C_1C_7H	112.4	115
$O_1{\cdots}H$	1.759				

[a] Dimerized monomer from crystal, ref 18.

been determined experimentally, the optimized geometry of TRN was calculated in order to determine how accurately the B3LYP/6-311+G(2d,p) method gave the observed structure. Table 1 compares the calculated bond lengths and bond angles with the observed ones determined by X-ray crystal analysis.[18] The numbering of the carbon and oxygen atoms is shown in Figure 1a. Most of the calculated bond lengths are in agreement with the experimentally observed ones. The largest discrepancy is seen in the length of the $O_2{-}H$ bond, which is longer than the observed length. The discrepancy would be due to the overestimation of the strength of hydrogen bond.[19,20] Bond alternation is observed for the calculated carbon−carbon bonds. Tropolone has a longer $C_1{-}C_2$ bond than the other formal C−C single bonds.[18] The same trend is reproduced in the present calculations. The calculation gives nearly equal bond lengths for the formal C=C double bonds, namely, $C_2{=}C_3$, $C_4{=}C_5$, and $C_6{=}C_7$. On the other hand, the crystal structure is shown to have a shorter bond length in the $C_4{=}C_5$ bond than in other C=C bonds. This discrepancy has been ascribed to the absence of the averaging effect of the bond lengths, as the $C_4{=}C_5$ bond is distant from the electron-attractive carbonyl group.[18] These results suggest that the conjugation effect between C=C double bonds tends to be overestimated in the B3LYP/6-311+G(2d,p) calculation. The same tendency has been observed in the optimized geometry of TRN by other ab initio methods.[20−24] The estimated C−H bond lengths are almost constant at 1.085 Å, a value which is in agreement with X-ray analysis data, except in the case of the C_4H bond. The observed bond length of 1.04 Å in the C_4H bond is shorter than expected, as compared with typical C−H bonds[25] of aromatic compounds.

There are appreciable disagreements between the calculated and observed values of some bond angles, namely, $C_1C_2O_2$, C_2O_2H, and C_1C_7H. These bond angles are adjacent to or neighboring the carbonyl group. The B3LYP method is known to overestimate the strength of hydrogen bonds.[19,20] This suggests that the hydroxyl proton is strongly attracted to the carbonyl oxygen. As a result bond angles $C_1C_2O_2$ and C_2O_2H would become smaller. The apparent narrowing in C_1C_7H could be explained as an overestimation of the electron-attracting character of the carbonyl group.

As stated above, some of the calculated bond lengths and bond angles are not in agreement with the observed values. However, it can be concluded that the B3LYP/6-311+G(2d,p) method can produce a good approximation of the observed structure.

3.1.2. Optimized Geometry of 5PTRN. It is possible that there are energy minima in the potential surface for the normal form of 5PTRN (I, Figure 1b), as well as for the tautomer form (II, Figure 1c), and the conformers (III and IV), which are due to the phenyl group rotation in I and II, respectively. The conformer III is converted into the conformer IV via proton transfer as well. The optimized geometries and their energies were then calculated for the four isomers. Table 2 indicates the energies and the torsional dihedral angles ϕ_1 and ϕ_2 between the tropolone and phenyl rings for the four isomers, where ϕ_1 and ϕ_2 stand for the dihedral angles of the C_4C_5 bond and the C_6C_5 bond to the phenyl ring, respectively. Figure 2 shows the side view of the four isomers, which have equivalent energy within the limits of the calculations. The corresponding bond lengths and bond angles of the four isomers had identical values within the accuracy of estimation, although the two dihedral angles were slightly different. The difference between the two torsional

TABLE 2: Dihedral Angles and Energies of Geometries with Equivalent Minima Calculated by the B3LYP/6-311+G(2d,p) Method

		dihedral angle (degree)		
geometry	state	ϕ_1	ϕ_2	energy (hartree)
I	(S_0)	44.1	44.2	−652.02849122
II	(S_0)	44.1	44.3	−652.02849093
III	(S_0)	−44.1	−44.3	−652.02849105
IV	(S_0)	−44.1	−44.3	−652.02849095

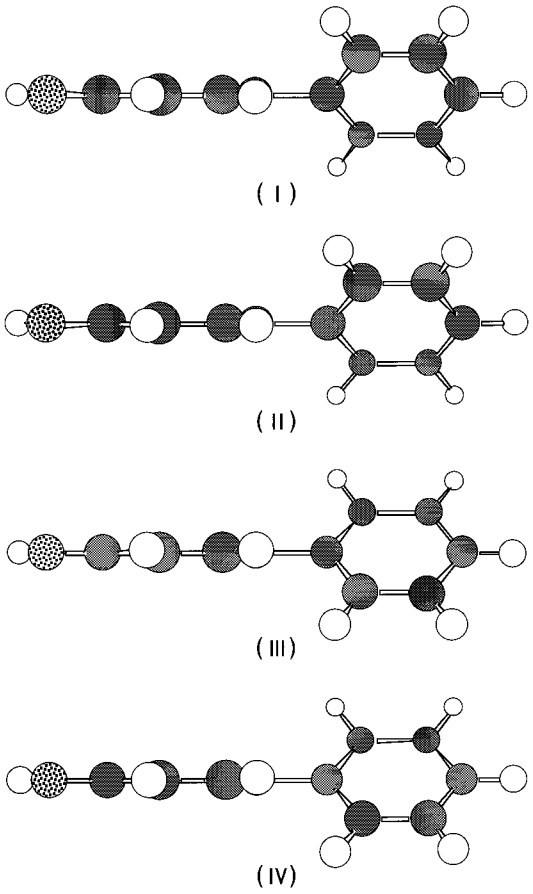

Figure 2. Side view of the four equivalent isomers in the S_0 state.

dihedral angles will be discussed later. These results suggest that due to proton transfer and phenyl ring rotation, there are four equivalent minima in the potential surface. Proton tunneling can occur between isomers I and II, and/or between isomers III and IV.

Figure 3 shows the bond lengths and the bond angles for the optimized geometry of the normal form. The numbering of the carbon and oxygen atoms is given in Figure 1b. Bond alternation is observed for carbon−carbon bonds in the tropolone skeleton. The C_1-C_2 bond is longer than the typical single bonds between carbon atoms, which is characteristic of tropolones.[18] As noted above, the optimization of TRN geometry gave almost equal bond lengths for all of the formal C=C double bonds because of the overestimation of the π-electron conjugation. In contrast, the formal double bond $C_4=C_5$ is longer than other double bonds $C_2=C_3$ and $C_6=C_7$ in 5PTRN, as shown in Figure 3. Substitution of the phenyl group at the 5-position causes the steric repulsion between nonbonded 1,4-hydrogen atoms bonded to carbon atoms C_4 and C_9, and also between 1,4-hydrogen atoms bonded to carbon atoms C_6 and C_{13} (these hydrogen atoms are abbreviated hereafter as H_4, H_9, H_6, and H_{13}, respectively, or simply are referred to as 1,4-hydrogen atoms). As a result, the

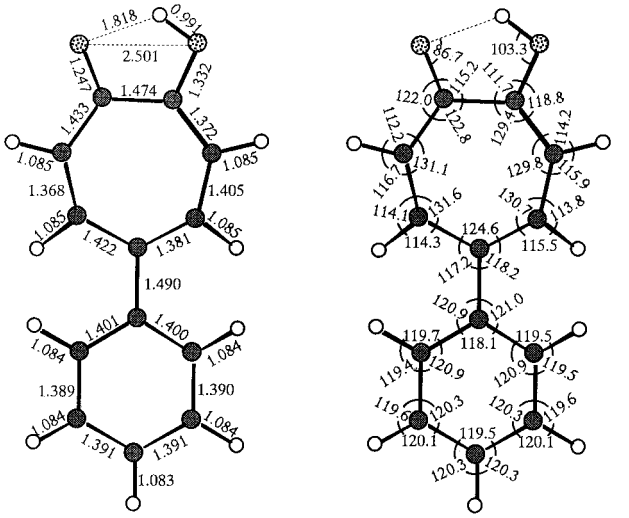

Figure 3. Bond lengths and bond angles for the optimized geometry of the normal form of 5PTRN in the S_0 state.

$C_4=C_5$ bond is elongated in order to release steric repulsion due to the 1,4-hydrogen atoms. This assumption is supported by the fact that the formal single bond C_5-C_6 becomes longer than that observed in the case of TRN. There is no appreciable difference in the O_2-H bond length, compared with that of TRN. However, the $O_1\cdots O_2$ and $O_1\cdots H$ distances become longer than those of TRN. They may be related to the elongation of the C_1-C_2 single bond and to the broadening of $C_2C_1O_1$ and $C_1C_2O_2$ bond angles in 5PTRN. Other bond lengths in the tropolone skeleton do not differ greatly from the corresponding bonds in the optimized geometry of TRN. An interesting feature of 5PTRN is the bond angle expansion, except for the bond angle $C_4C_5C_6$, which is smaller by 3° than that of TRN. The shrinkage of the bond angle $C_4C_5C_6$ is probably due to the steric repulsion between nonbonded 1,4-hydrogen atoms, as mentioned above.

As regards the phenyl ring, the C_8-C_9 and C_8-C_{13} bonds become longer than other C−C bonds close to those of aromatics.[25] This effect is also due to steric repulsion between nonbonded 1,4-hydrogen atoms. The bond lengths of the C−H bonds and the bond angles in the phenyl ring are similar to those of aromatics.[26]

As shown in Table 2, the torsional dihedral angles between the two rings ϕ_1 and ϕ_2 are slightly different in the all of the four isomers. If the tropolone skeleton in 5PTRN is planar, the two torsional dihedral angles are expected to be equal. The dihedral angles between in-ring carbon atoms indicate that the tropolone skeleton takes a slightly nonplanar configuration. A small difference between the two torsional dihedral angles is due to the nonplanar structure of the tropolone skeleton. However, the difference in the two torsional dihedral angles is very small. We may treat the seven-membered ring of the tropolone moiety as assuming an approximately planar conformation in the S_0 state, and the equilibrium torsional dihedral angle (ϕ) is assumed to be ca. 44°. The torsional dihedral angle has been observed to be 47 ± 1° for 5PTRN(−OD), the isotopomer of 5PTRN, in which the hydroxyl proton is deuterated.[13] Since the potential surface does not appreciably change upon deuteration of the hydroxyl proton, it can be concluded that the dihedral angle of ca. 44° calculated by the B3LYP/6-311+G(2d,p) method gives the value close to the equilibrium torsional dihedral angle of 5PTRN.

3.1.3. Geometry of the Transition State for Proton Transfer. The optimized geometries of the isomers and their energies

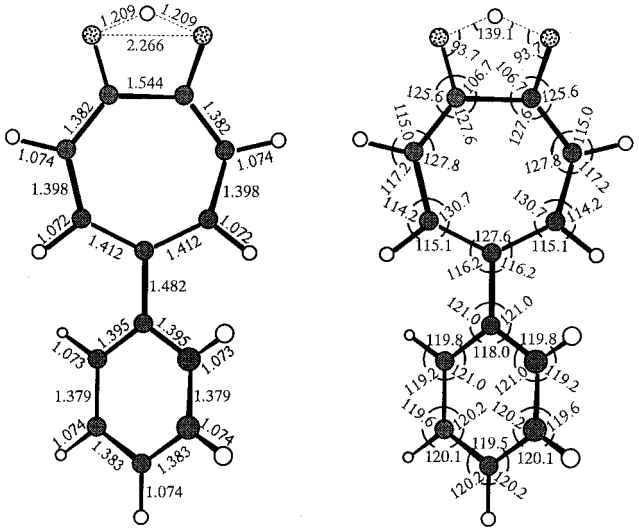

Figure 4. Bond lengths and bond angles in the transition state for proton transfer in the S_0 state.

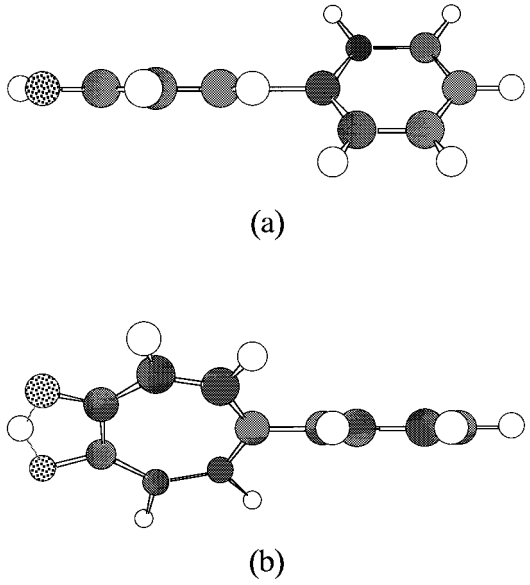

Figure 5. Side view of the geometry in the transition state for proton transfer in the S_0 state.

suggest that proton tunneling can occur between the tautometric isomers. As the structure of the transition state for proton transfer is of interest, we calculated the geometry of the transition state for proton transfer. Figure 4 indicates the bond lengths and bond angles of the transition state. The side views of the geometry of the transition state are shown in Figure 5. Both the tropolone ring moiety and the phenyl ring are planar, and the former takes a structure close to the C_{2v} symmetry. The bond lengths in the C_4-C_5 and C_5-C_6 bonds are longer than other C−C bonds in the tropolone skeleton. The dihedral angle between the two rings was 45°. Furthermore, the carbon atoms C_5, C_8, and C_{11} were collinear. These results suggest that the tropolone moiety has the geometry close to the C_{2v} symmetry in the transition state, irrespective of the presence of the phenyl ring. The torsional dihedral angle between the tropolone and phenyl rings increases slightly in the transition state for proton transfer.

3.1.4. Vibrational Modes and Frequencies. Due to the calculation capacity of our machine, vibrational modes and frequencies were calculated using the B3LYP/6-31G** level of theory. The calculation of normal modes was carried out without consideration of tunneling or of potential function anharmonicity. A three-dimensional displacement of atoms was seen in all of the vibrational modes because of the nonplanar structure of 5PTRN. The O−H stretching vibration was calculated to be 3317 cm^{-1}. The calculated O−H stretching vibration for TRN was 3295 cm^{-1} at the same level of calculation, and the observed frequency has been reported to be 3121 cm^{-1}.[27,28] The ratio of observed/calculated frequency is 0.947. If we apply the same scaling factor to the O−H stretching vibration of 5PTRN, the frequency is reduced to 3140 cm^{-1}.

The calculation gave the fundamentals of 55, 62, 101, 135, and 185 cm^{-1} in the low-frequency region. The fundamentals of 55, 62, and 135 cm^{-1} have been correlated to the observed fundamentals of 53, 59, and 124 cm^{-1}.[13] Among them, the only clear assignment has been performed for the fundamental of 59 cm^{-1}, which is ascribed to phenyl torsion. The observed fundamentals of 53 and 124 cm^{-1} have been assigned tentatively to mode A and mode B, respectively.[13] Examination on the vibrational mode of the calculated fundamental of 55 cm^{-1} leads to the assignment that mode A is due to the skeletal/COH wagging vibration in the tropolone moiety, which is accompanied by an out-of-plane CH bending vibration in the phenyl ring (phenyl flapping). Similarly, mode B can be assigned to the skeletal/OCCO twisting vibration in the tropolone moiety, which is accompanied with an out-of-plane CH bending vibration in the phenyl ring.

Apart from the three fundamentals assigned above, we found low-frequency fundamentals of 93 and 176 cm^{-1}, but these fundamentals had not been assigned in our previous paper.[13] The calculated fundamental of 101 cm^{-1} is ascribed to the in-plane bending mode between the phenyl ring and the tropolone ring. The observed fundamental of 93 cm^{-1} can be correlated to this mode of vibration. The calculated fundamental of 185 cm^{-1} can be attributed to the skeletal/COH wagging vibration in the tropolone moiety, which is accompanied by an out-of-plane CH bending vibration in the phenyl ring. The fundamental for the skeletal/COH wagging vibration has been reported to be 177 cm^{-1} for TRN.[27−29] Hence, we assigned the fundamental of 176 cm^{-1} to a skeletal/COH wagging vibration in the tropolone moiety accompanied by an out-of-plane CH bending vibration in the phenyl ring. In TRN, the fundamentals for the skeletal/OCCO twisting vibration, ν_{26}, and the skeletal/COH wagging vibration, ν_{25}, have been reported to be 110 and 177 cm^{-1}, respectively.[27−29] The present results imply that the skeletal/OCCO twisting vibration is affected by the substitution of the phenyl group, but the skeletal/COH wagging vibration is not similarly affected. From the comparison of the ratios of the observed/calculated frequency for the low-frequency bands assigned above, the average scaling factor is assumed to be 0.941.

3.1.5. Barrier for Phenyl Torsion. Proton tunneling is associated with phenyl ring torsion.[13] We calculated the energy dependence of the conformers on phenyl ring rotation about the C_5-C_8 bond. The energies were estimated by fixing the torsional angle, ϕ, every 10 degrees from 0° to 180°. Here, the torsional angle ϕ_1 refers to the torsional angle ϕ. Figure 6 indicates the torsional angle dependence of conformation energies relative to that of the conformation at $\phi = 0°$. There are two barriers at $\phi = 0°$ and $\phi = 90°$; the barrier height of the latter (1260 cm^{-1}) is lower than that of the former (620 cm^{-1}). Barrier heights have been determined experimentally to be 920 and 710 cm^{-1} at $\phi = 0°$ and $\phi = 90°$, respectively, for 5PTRN(−OD).[13] The torsional potential is assumed to differ little between 5PTRN and 5PTRN(−OD). The barrier heights

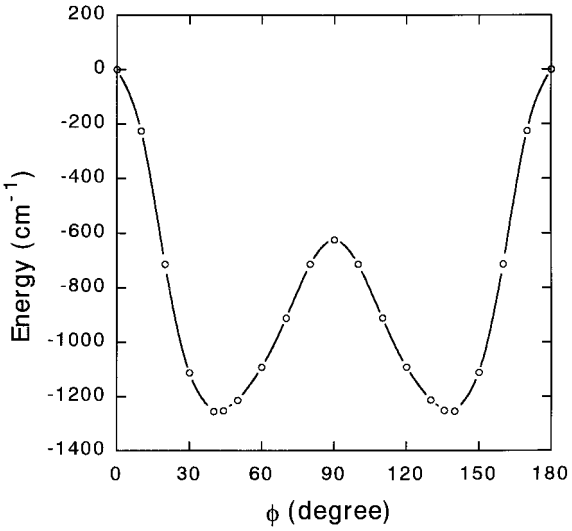

Figure 6. Torsional angle dependence of conformation energies in the S_0 state, relative to that of conformation at $\phi = 0$. (a) ○: energies calculated by the B3LYP/6-311+G(2d,p) method; (b) −−: the best fit curve ($V_2 = -407$ cm^{-1}, $V_4 = -939$ cm^{-1}, $V_6 = -217$ cm^{-1}, $V_8 = -111$ cm^{-1}).

for phenyl torsion are not affected by substituting a deuterium atom for a hydroxyl proton. It is possible to compare the calculated barrier heights with the observed values for 5PTRN(−OD). The B3LYP/6-311+G(2d,p) level of theory is determined to give a barrier height close to the observed one at $\phi = 90°$ but to overestimate the height at $\phi = 0°$. The calculation probably overestimates the steric repulsion between nonbonded 1,4-hydrogen atoms.

The barrier heights at $\phi = 0°$ and $\phi = 90°$ have been determined to be 125 and 175 cm^{-1}, respectively, in the S_0 torsional potential of biphenyl.[32] The heights of the both barriers are much smaller than those of 5PTRN. One reason for this difference would be the greater steric repulsion between nonbonded 1,4-hydrogen atoms in 5PTRN than would occur in biphenyl. This finding suggests that the phenyl ring is more difficult to rotate around the seven-membered ring than around the six-membered ring.

The torsional energy levels can be calculated from the torsional potentials, $V(\phi)$. The calculated potential energies were fitted to an eq 1, to obtain the potential parameters, $V_n (n = 2, 4, 6, 8)$:

$$V(\phi) = 1/2[V_2(1 - \cos 2\phi) + V_4(1 - \cos 4\phi) + V_6(1 - \cos 6\phi) + V_8(1 - \cos 8\phi)] \quad (1)$$

The smooth curve in Figure 6 demonstrates the best fitting curve. The potential parameters were determined to be -407 ± 14 cm^{-1} (V_2), -939 ± 12 cm^{-1} (V_4), -217 ± 14 cm^{-1} (V_6), and -111 ± 12 cm^{-1} (V_8). The torsional energies were calculated by the method of Lewis et al.[30] The internal rotational constant B was calculated by the method of Pitzer,[31] with the geometry optimized by the ab initio calculation. Table 3 shows the torsional energy levels calculated by the B3LYP/6-311+G(2d,p) method together with those calculated by the B3LYP/6-31G** method. The fundamental for phenyl torsion has been determined to be 59 cm^{-1} in the case of 5PTRN(−OD).[13] The B3LYP/6-311+G(2d,p) method gives lower torsional energy levels than the observed levels for 5PTRN(−OD). Interestingly, the calculation at the 6-31G** level reproduces the experimental values rather well.

TABLE 3: Torsional Energy Levels of 5PTRN in the S_0 State

ν''	B3LYP 6-311+G(2d,p) (cm^{-1})	B3LYP 6-31G** (cm^{-1})	obs.[a] (cm^{-1})
1	53	60	59
2	104	118	118
3	155	175	174
4	205	231	231
5	254	286	288
6	304	340	342

[a] Reference 13.

TABLE 4: Dihedral Angles and Energies of Geometries with Equivalent Minima Calculated by the CIS/ 6-311+G(2d,p) Method

		dihedral angle (degree)		
geometry	state	ϕ_1	ϕ_2	energy (hartree)
I	(S_1)	26.7	27.1	−647.83546062
II	(S_1)	26.8	27.2	−647.83546046
III	(S_1)	−26.7	−27.1	−647.83546061
IV	(S_1)	−26.7	−27.0	−647.83545988

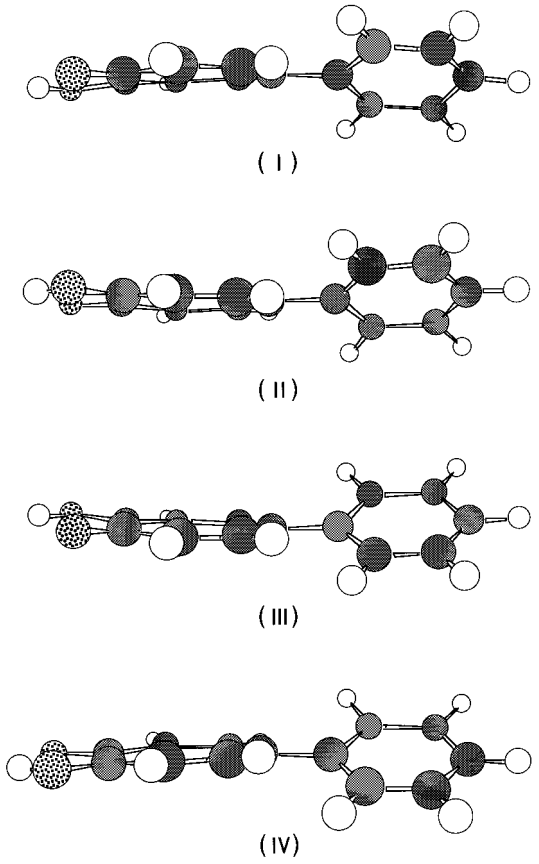

Figure 7. Side view of the four equivalent isomers in the S_1 state.

3.2. Calculation for the S_1 State. Table 4 lists the energies and the torsional dihedral angles ϕ_1 and ϕ_2 for the four isomers that are the result of proton transfer and phenyl ring rotation. Figure 7 shows the side views of these isomers. The energies of the isomers are identical within the accuracy of the calculations. The four isomers have identical values for the corresponding bond lengths and bond angles in both the tropolone moiety and the phenyl ring. Although the nonplanarity of the tropolone moiety increases, as will be mentioned later, the results suggest that there are four equivalent minima in the potential surface. As is clear from Figure 7, the tropolone moiety reverses

TABLE 5: Optimized Geometries of 5PTRN in the S_0 and S_1 State at the 6-311+G(2d,p) Level

	bond length (Å)			bond angle (degree)	
	S_1 (CIS)	S_0 (HF)		S_1 (CIS)	S_0 (HF)
$C_1{=}O_1$	1.210	1.207	$C_2C_1{=}O_1$	116.2	116.5
$C_2{-}O_2$	1.325	1.328	$C_1C_2{-}O_2$	114.9	112.8
O_2H	0.951	0.951	C_2O_2H	108.0	107.5
C_1C_2	1.465	1.479	$C_1C_2C_3$	128.2	128.6
C_2C_3	1.389	1.341	$C_2C_3C_4$	130.5	130.7
C_3C_4	1.373	1.429	$C_3C_4C_5$	130.2	130.7
C_4C_5	1.441	1.346	$C_4C_5C_6$	124.5	124.5
C_5C_6	1.412	1.440	$C_5C_6C_7$	131.8	131.5
C_6C_7	1.360	1.341	$C_6C_7C_1$	129.9	131.1
C_7C_1	1.458	1.450	C_4C_3H	115.9	115.0
C_5C_8	1.457	1.496	C_5C_4H	115.5	116.0
C_8C_9	1.406	1.388	$C_6C_5C_8$	118.4	116.6
C_9C_{10}	1.379	1.383	C_7C_6H	113.3	114.3
$C_{10}C_{11}$	1.380	1.381	C_1C_7H	112.0	111.7
$C_{11}C_{12}$	1.390	1.383	$C_5C_8C_9$	121.0	120.9
$C_{12}C_{13}$	1.371	1.381	$C_8C_9C_{10}$	121.4	120.8
$C_{13}C_8$	1.409	1.390	$C_9C_{10}C_{11}$	120.5	120.3
C_3H	1.075	1.075	$C_{10}C_{11}C_{12}$	119.2	119.5
C_4H	1.071	1.075	$C_{11}C_{12}C_{13}$	120.6	120.2
C_6H	1.073	1.075	$C_{12}C_{13}C_8$	121.4	120.8
C_7H	1.073	1.075	$C_{13}C_8C_9$	116.8	118.4
C_9H	1.072	1.074	C_8C_9H	120.0	119.6
$C_{10}H$	1.074	1.075	$C_9C_{10}H$	119.4	119.6
$C_{11}H$	1.074	1.074	$C_{10}C_{11}H$	120.5	120.3
$C_{12}H$	1.074	1.075	$C_{11}C_{12}H$	119.9	120.1
$C_{13}H$	1.072	1.075	$C_{12}C_{13}H$	118.4	119.8
$O_1{\cdots}O_2$	2.561	2.536	$C_4C_5C_8C_9$	26.7	52.1
$O_1{\cdots}H$	2.013	1.960	$C_6C_5C_8C_{13}$	27.1	52.2

the configuration relative to the phenyl ring via proton transfer. Table 5 lists the bond lengths and bond angles for the normal form in the S_1 state by using the CIS method at the 6-311+G(2d,p) level. Structural parameters of the S_1 state were compared with those of the S_0 state by using the HF level of calculation, because the B3LYP calculation cannot be applied in the case of the S_1 state. In the S_0 state, the $C_2{-}C_3$, $C_4{-}C_5$, and $C_6{-}C_7$ bonds were doubly bonded and there exists bond alternation between the carbon−carbon bonds in the seven-membered ring of the tropolone moiety. On the other hand, in the S_1 state, the $C_2{-}C_3$ and $C_3{-}C_4$ bonds have similar bond lengths, which are intermediate between the typical single and double C−C bonds of conjugated systems.[25] The same tendency has been observed in the S_1 state in TRN.[20−24] The nonbonded O···O and O···H distances are longer than those calculated for the S_0 state. This finding is in contrast to the case of TRN in which both the O···O and O···H distances become shorter upon excitation to the S_1 state.[20−22,24]

The equilibrium torsional dihedral angles ϕ_1 and ϕ_2 are calculated to be 26.7° and 27.1°, respectively, for the normal form, as shown in Table 4; these values are about one-half of the values calculated in the S_0 state. The calculations indicated that dihedral angles between carbon atoms in the tropolone skeleton increased to 2.5 ∼ 5.5°, except in the case of $C_2C_3C_4C_5$; the deviation from the planarity was also considerably larger in the tropolone skeleton, compared to that of the S_0 state. As a result, the torsional dihedral angles ϕ_1 and ϕ_2 are slightly different, but their difference is small. Furthermore, C_5, C_8, and C_{12} atoms do not lie along the same line, suggesting that 5PTRN takes a bent structure in the S_1 state, as shown in Figure 7. The bending direction of the tropolone moiety changed, depending on the angle of phenyl torsion. A bent structure would support the hypothesis suggested in our previous paper that phenyl torsion suppresses proton tunneling.[13] The torsional dihedral angle is determined by the balance between the π-electron conjugation through the two rings and the steric repulsion due to the nonbonded 1,4-hydrogen atoms. The decrease in the torsional dihedral angle suggests an increase in the contribution of the π-electron conjugation in the S_1 state.

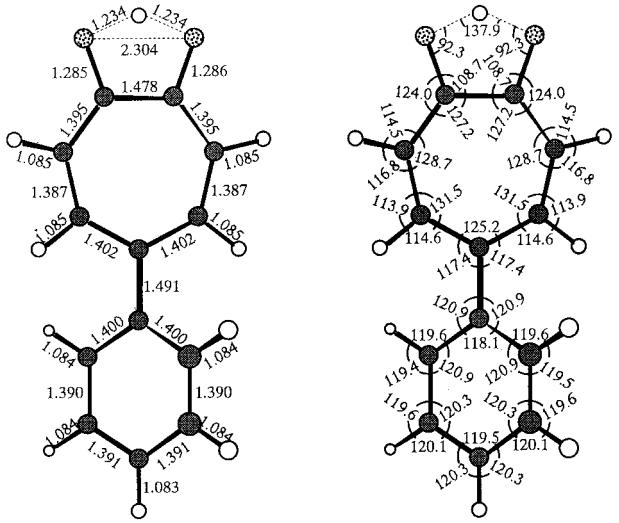

Figure 8. Bond lengths and bond angles in the transition state for proton transfer in the S_1 state.

A comparison of the torsional angle between the two phenyl rings in the S_1 state of biphenyl is also of interest. In contrast to 5PTRN, the two phenyl rings take a coplanar conformation in the S_1 state of biphenyl.[32,33] The torsional angles of 5PTRN indicate that the contribution of the ϕ-electron conjugation is not large enough to take the coplanar conformation due to the great steric hindrance caused by nonbonded 1,4-hydrogen atoms between the two rings. This steric repulsion contributes to an increase in the nonplanarity in the tropolone skeleton in the S_1 state as well.

Tunneling splitting has been reported to be about 18 cm^{-1} in the 0_0^0 transition, suggesting that 5PTRN has a double-well potential along the H···O···H coordinates in the S_1 state.[13] The calculation suggests that the tautomer has the same energy and structural parameters as the normal form, implying that 5PTRN has a double-well potential along the H···O···H coordinates in the S_1 state. The structure of the transition state for proton transfer is of interest at this juncture. Figure 8 shows the bond lengths and the bond angles of the transition state. Figure 9 indicates the side views of the geometry of the transition state. The hydroxyl proton is equidistant from the O_1 and O_2 oxygen atoms. Bond lengths and angles are symmetrical with respect to the axis connecting the hydroxyl proton and the C_{11} atom. The two torsional dihedral angles are equal at 39.6°. Figure 9 suggests that the tropolone ring moiety is nearly planar. Furthermore, the carbon atoms C_5, C_8, and C_{11} are collinear. These results suggest that the tropolone moiety changes the geometry close to the C_{2v} symmetry in the transition state for proton transfer. It should be noted that the torsional dihedral angle in the transition state increases to 39.6°, which is in contrast to the S_0 state. Figure 10 shows the dependence of relative potential energies of the conformers on the rotational angle of the phenyl group. Relative potential energies are calculated at the 6-31G** level, because the calculation at the 6-311+G(2d,p) level could not be carried out at $\phi = 0°$. Since the CIS method overestimates the excitation energies due to its insufficient treatment of electron correlation effects, the qualitative information on torsional potential is given for the S_1 state. The barrier height at $\phi = 0°$ becomes smaller than that at $\phi = 90°$, a finding which is reversed in the case of the S_0 state.

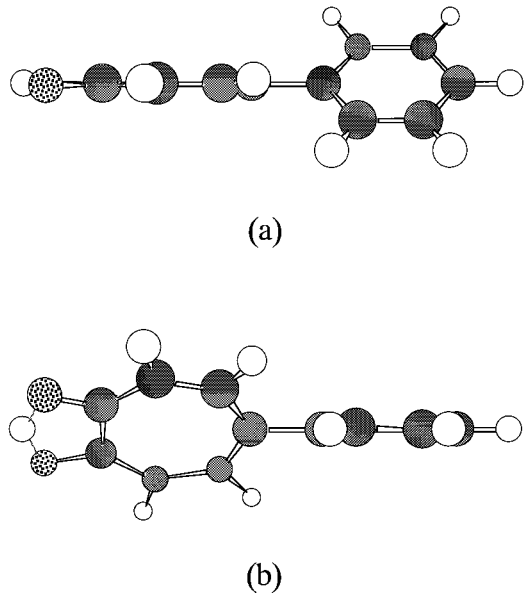

Figure 9. Side view of the geometry in the transition state for proton transfer in the S_1 state.

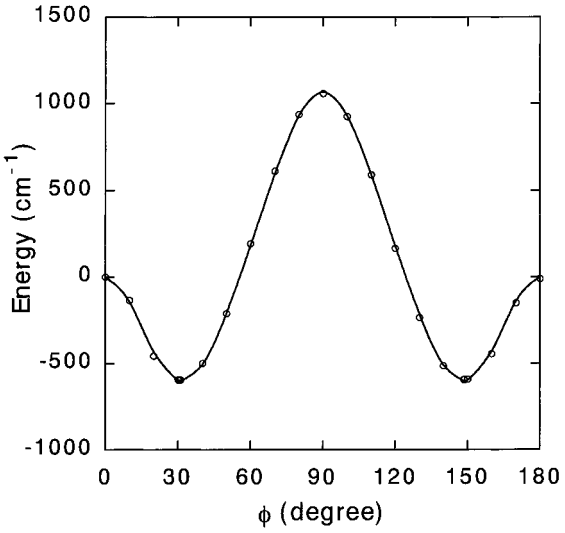

Figure 10. Torsional angle dependence of conformation energies in the S_1 state, relative to that of conformation at $\phi = 0$. (a) ○: energies calculated by the CIS/6-31G** method; (b) −−: the best fit curve (V_2 = 1230 cm^{-1}, $V_4 = -911$ cm^{-1}, $V_6 = -163$ cm^{-1}, $V_8 = -77$ cm^{-1}).

4. Conclusion

The optimized geometries of 5PTRN were calculated in the S_0 and S_1 states, by using the B3LYP and CIS methods, respectively, at the 6-311+G(2d,p) level. It was concluded that the B3LYP/6-311+G(2d,p) method afforded the accurate structure of the S_0 state of 5PTRN. The tropolone moiety deviated only slightly from planarity in the S_0 state, but it was assumed to have been a planar structure. The equilibrium torsional dihedral angle in the S_0 state was determined to be ca. 44 °, which is close to that of 5PTRN(−OD). As regards the S_1 state, the nonplanarity of the tropolone skeleton increased and thus assumed a bent structure, which supported the experimental findings. Furthermore, the equilibrium torsional dihedral angle became smaller than that in the S_0 state, suggesting an increase in the contribution of the π-electron conjugation in the S_1 state. There were four equivalent isomers due to proton transfer and phenyl rotation in both the S_0 and S_1 states. In agreement with the experimental observations, these results suggested that proton tunneling could occur in 5PTRN. The geometry in the transition state was calculated by the QST2 method. The calculations gave interesting information that the tropolone moiety had a structure close to the C_{2v} symmetry in both the S_0 and S_1 states, although the S_1 state was assumed to have a bent structure. There were two barriers at $\phi = 0°$ and 90° for phenyl torsion, and their relative heights were reversed in the S_1 state. Normal vibrational modes were determined by the B3LYP method for the S_0 state. The observed bands in the low frequency region could be successfully assigned based on calculations.

Acknowledgment. The authors gratefully acknowledge a Grant-in-Aid for Priority-Area-Research "Photodissociation Dynamics" from the Ministry of Education, Science, and Culture of Japan for the support of this study.

References and Notes

(1) Tsuji, T.; Sekiya, H.; Nishimura, Y.; Mori, R.; Mori, A.; Takeshita, H. *J. Chem. Phys*. **1992**, *97*, 6032.

(2) Sekiya, H.; Sasaki, K.; Nishimura, Y.; Mori, A.; Takeshita, H. *Chem. Phys. Lett*. **1990**, *174*, 13.

(3) Tsuji, T.; Sekiya, H.; Ito, S.; Ujita, H.; Habu, M.; Mori, A.; Takeshita, H.; Nishimura, Y. *Rep. Inst. Adv. Mater. Study, Kyushu Univ*. **1993**, *7*, 1.

(4) Ensminger, F. A.; Plassard, J.; Zwier, T. S. *J. Phys. Chem*. **1993**, *97*, 4344.

(5) Ensminger, F. A.; Plassard, J.; Zwier, T. S.; Hardinger, S. *J. Chem. Phys*. **1993**, *99*, 8341.

(6) Ensminger, F. A.; Plassard, J.; Zwier, T. S.; Hardinger, S. *J. Chem. Phys*. **1995**, *102*, 5246.

(7) Nash, J. J.; Zwier, T. S.; Jordan, K. D. *J. Chem. Phys*. **1995**, *102*, 5260.

(8) Pazz, J. J.; Moreno, M.; Lluch, J. M. *J. Chem. Phys*. **1997**, *107*, 6275.

(9) Pazz, J. J.; Moreno, M.; Lluch, J. M. *J. Chem. Phys*. **1998**, *108*, 8114.

(10) Nishi, K.; Sekiya, H.; Kawakami, H.; Mori, A.; Nishimura, Y. *J. Chem. Phys*. **1998**, *109*, 1589.

(11) Nishi, K.; Sekiya, H.; Kawakami, H.; Mori, A.; Nishimura, Y. *J. Chem. Phys*. **1999**, *111*, 3961.

(12) Tsuji, T.; Hayashi, Y.; Sekiya, H.; Hamabe, H.; Nishimura, Y.; Kawakami, H.; Mori, A. *Chem. Phys. Lett.* **1997**, *278*, 49.

(13) Tsuji, T.; Hayashi, Y.; Hamabe, H.; Kawakami, H.; Mori, A.; Nishimura, Y.; Sekiya, H. *J. Chem. Phys*. **1998**, *110*, 8485.

(14) Frisch, M. J.; Trucks, G. W.; Schlegel, H. B.; Gill, P. M. W.; Johnson, B. G.; Robb, M. A.; Cheeseman, J. R.; Keith, T.; Petersson, G. A.; Montgomery, J. A.; Raghavachari, K.; Al-Laham, M. A.; Zakrzewski, V. G.; Ortiz, J. V.; Foresman, J. B.; Cioslowski, J.; Stefanov, B. B.; Nanayakkara, A.; Challacombe, M.; Peng, C. Y.; Ayala, P. Y.; Chen, W.; Wong, M. W.; Andres, J. L.; Replogle, E. S.; Gomperts, R.; Martin, R. L.; Fox, D. J.; Binkley, J. S.; Defrees, D. J.; Baker, J.; Stewart, J. P.; Head-Gordon, M.; Gonzalez, C.; Pople, J. A. *Gaussian 94*, revision E.2; Gaussian, Inc.: Pittsburgh, PA, 1995.

(15) (a) Becke, A. *J. Chem. Phys*. 1993, *98*, 1372, 5648. (b) Lee, C.; Yang, W.; Parr, R. G. *Phys. Rev. B* **1988**, *41*, 785.

(16) Frisch, M. J.; Pople, J. A.; Binkey, J. S. *J. Chem. Phys*. **1984**, *80*, 3265.

(17) Foresman, J. B.; Head-Gordon, M.; Pople, J. A.; Frisch, M. J. *J. Phys. Chem*. **1992**, *96*, 135.

(18) Shimanouchi, H.; Sasada, Y. *Acta Crystallogr*. **1973**, B, *29*, 81.

(19) Becke, A. *J. Chem. Phys*. **1988**, *88*, 1053.

(20) Smerdarchina, Z.; Siebrand, W.; Zgierski, M. Z. *J. Chem. Phys*. **1996**, *104*, 1203.

(21) Vener, M. V.; Scheiner, S.; Sokolov, N. D. *J. Chem. Phys*. **1994**, *101*, 9755.

(22) Pazz, J. J.; Moreno, M.; Lluch, J. M. *J. Chem. Phys*. **1995**, *103*, 353.

(23) Wójcik, M. J.; Nakamura, H.; Iwata, S.; Tatara, W. *J. Chem. Phys*. **2000**, *112*, 6322.

(24) Nishimura, Y. unpublished data.

(25) Lide, D. R., Ed. *CRC Handbook of Chemistry and Physics*, 73rd ed; CRC Press: Boca Raton, 1992.

(26) Almenpingen, A.; Bastiansen, O. K. *Nor. Videnski. Selsk*. **1958**, *4*, 1.

(27) Redington, R. L.; Redington, T. E. *J. Mol. Spectrosc*. **1979**, *78*, 229.

(28) Redington, R. L.; Bock, C. W. *J. Phys. Chem*. **1991**, *95*, 10284.

(29) Sekiya, H.; Nagashima, Y.; Nishimura, Y. *J. Chem. Phys*. **1990**, *92*, 1761.

(30) Lewis, L. D.; Malloy, T. B., Jr.; Chao, T. H.; Laane, J. *J. Mol. Struct*. **1972**, *12*, 427.

(31) Pitzer, K. S.; Gwinn, W. D. *J. Chem. Phys*. **1942**, *10*, 428. Pitzer, K. S. *J. Chem. Phys*., **1946**, *14*, 239.

(32) Murakami, J.; Ito, M.; Kaya, K. *J. Phys. Chem*. **1981**, *74*, 6505.

(33) Im, H.-S.; Bernstein, E. R. *J. Chem. Phys*. **1988**, *88*, 7337.